Available online at www.sciencedirect.com
SCIENCE DIRECT®
Tetrahedron: Asymmetry
Tetrahedron: *Asymmetry* 16 (2005) 25–32

Crystallographic analysis of the interactions of *Drosophila melanogaster* Golgi α-mannosidase II with the naturally occurring glycomimetic salacinol and its analogues

Douglas A. Kuntz,[a] Ahmad Ghavami,[b] Blair D. Johnston,[b] B. Mario Pinto[b,*] and David R. Rose[a,*]

[a]*Ontario Cancer Institute and Department of Medical Biophysics, University of Toronto, 610 University Avenue, Toronto, Ontario, Canada M5G 2M9*
[b]*Department of Chemistry, Simon Fraser University, Burnaby, Canada BC V5A 1S6*

Received 19 October 2004; accepted 22 November 2004
Available online 24 December 2004

Abstract—Golgi α-mannosidase II, a component of the *N*-glycosylation pathway and a member of glycosyl hydrolase family 38, is an attractive target for inhibition with anti-tumor or anti-inflammatory outcomes. This enzyme operates via the classical two-step catalytic mechanism of retaining glycosidases. Recently, a novel, general class of glycosidase inhibitors has been developed based on the natural anti-diabetic compound, salacinol. Previously, these inhibitors have shown activity against intestinal α-glucosidases, glucoamylase, and α-amylase. Herein, we investigate by X-ray crystallography, the interactions of these compounds with Golgi α-mannosidase II, and compare these interactions with those of the naturally occurring inhibitor, swainsonine. The mode of interaction of analogues of salacinol to α-mannosidase II is distinct from that described previously for glucosidases. The results demonstrate the ability of these general glycosidase inhibitors to interact with enzymes of a wide range of structures, and shed light on the general binding properties of α-mannosidase II. Specifically, they highlight the importance of octahedral coordination to the active site zinc atom for good inhibition, and the ability of even these weak inhibitors to form critical interactions with active site carboxylates and, by virtue of their permanent positive charge, to simulate the oxacarbenium nature of the transition state.

1. Introduction

Golgi α-mannosidase II (GMII) is a key component of the *N*-glycosylation pathway in protein synthesis. Following the requisite processing by *N*-acetylglucosaminyl transferase I (GnTI), this family 38 glycosyl hydrolase cleaves both the α-(1→3) and α-(1→6) terminal mannoses from the (1→6) branch of the *N*-acetyl-glucosamine-(mannose)$_5$-(*N*-acetyl-glucosamine)$_2$ intermediate, in preparation for the action of *N*-acetylglucosaminyl transferase II (GnTII), the subsequent enzyme in the pathway. This pathway is associated with embryonic expression of α-(1→6) linked carbohydrate structures, and with their re-expression on metastatic tumor cells. Inhibition of GMII by swainsonine has shown promise in clinical trials as an anti-metastatic agent by interfering with the expression of complex carbohydrates. In order to contribute toward the discovery of highly specific and effective GMII inhibitors as a potential new class of anti-cancer agents, we have reported previously the atomic structure by X-ray crystallography of the *Drosophila* homologue of GMII (dGMII) and its complex with swainsonine **1** (numbers in bold refer to Chart 1) and other inhibitors.[1] We report here the structural analysis of dGMII complexed with a series of novel inhibitors **3**–**6** related to a naturally occurring glycosidase inhibitor, salacinol **2** (Chart 1).

In view of the difficulty in producing sufficient amounts of the mammalian GMII either by recombinant DNA technology or purification from tissue, study of the dGMII has provided a tractable model of the structural and functional features of GMII. The structure of the 1032-amino acid residue catalytic domain of dGMII is a globular domain separable on the basis of predominant secondary structural elements into an all-β and a mixed α/β sub-domain. A Zn atom sits in the active site,

* Corresponding authors. Tel.: +1 604 291 4884; fax: +1 604 291 5424 (B.M.P.); tel.: +1 416 946 2970; fax: +1 416 946 6529 (D.R.R.); e-mail addresses: bpinto@sfu.ca; drose@oci.utoronto.ca

0957-4166/$ - see front matter © 2004 Elsevier Ltd. All rights reserved.
doi:10.1016/j.tetasy.2004.11.057

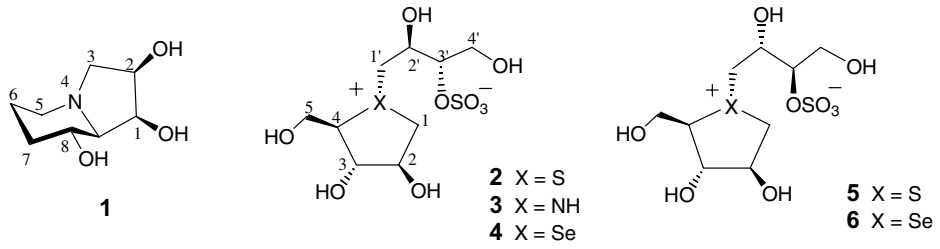

Chart 1. Inhibitors discussed in the text. Bolded numbers refer to the compounds throughout the text. Small numbers indicate the atomic numbering scheme.

in a cleft within the α/β sub-domain, and plays a role in binding inhibitors[1] and catalytic intermediates.[2]

GMII operates by the classical two-step mechanism of glycosyl hydrolases, in which the product retains the anomeric configuration of the substrate at the active C1 position.[3] In this mechanism, the reaction passes through an oxacarbenium-like transition state into a glycosylated covalent intermediate with the nucleophilic side chain of Asp 204, followed by a second similar transition state, leading to release of the product. As with other retaining glycosidases, a covalent intermediate can be stabilized and characterized crystallographically in dGMII with modified substrate or enzyme.[2]

The mimicry of carbohydrates by glycomimetics is an intriguing approach to deriving potential specific glycosidase inhibitors. Recently, a new class of glycosidase inhibitor with an intriguing inner-salt sulfonium–sulfate structure was isolated from the roots and stems of the plant *Salacia reticulata*.[4,5] Extracts of this plant have been traditionally used in the Ayurvedic method of Indian medicine as a treatment for type 2 diabetes. One of the active ingredients of these extracts is the sulfonium salt, salacinol **2**. Herein, we discuss our observations from the structural analysis of dGMII complexed with a series of inhibitors **3**–**6** related to salacinol **2**. Comparison of the interactions of the enzyme with a diastereoisomer **5** of salacinol, nitrogen **3**, and selenium **4** and **6** congeners, and swainsonine **1** explains the binding properties of these inhibitors to dGMII and provides information on further characteristics of the binding site that will be useful in the design of new inhibitors.

2. Results

The ability of salacinol **2** and its various analogues to inhibit Golgi mannosidase II was determined at the pH optimum of the enzyme (pH 5.75) using PNP–mannopyranoside as the artificial substrate. Although too weak for full K_i analyses with the amounts of material available, all analogues with salacinol-like stereochemistry at positions 2 and 3 proved to be weak inhibitors of the enzyme with IC_{50} values of approximately 7.5 mM. The stereochemistry of the aliphatic arm did not have an effect on the inhibition nor did the nature of the atom at the central position; sulfur, selenium, or nitrogen all behaved equally. The stereochemistry at positions C2 and C3 was critical for binding; the stereoisomers of salacinol at these positions were not inhibitory.

Despite the poor inhibitory activity of salacinol and its analogs we were interested to see whether we could visualize these compounds bound in the active site of GMII. Complexes in the crystal were formed by co-crystallization, where possible, or by soaking into crystals of unliganded protein. As well, the poor binding capabilities of this series of inhibitors necessitated incorporating the compounds into the cryoprotectant solution in order to obtain unambiguous electron density. Diffraction data and refinement statistics are summarized in Table 1.

The electron density for salacinol **2** and compounds **3**–**6** are shown in the simulated annealing F_o–F_c omit maps presented in Figure 1A–E. Figure 1E is a stereoview of compound **6** (seleno-salacinol diastereomer), the best defined of this series of inhibitors. The electron density for the five-membered ring is clear for each of the compounds. Examination of the structures of the complex of GMII with **2**–**6** indicates that the compounds are bound in an envelope conformation in the active site (Fig. 1).

The aliphatic arms of compounds **2** and **4** show no continuous electron density, but it is possible to infer the positions of the heavier S and O atoms from individual electron density peaks of appropriate size (Fig. 1A and C). The electron density for the aliphatic arms of diastereomers **5** and **6** was clearer than of those of salacinol or **4**. Only the nitrogen analog **3** had well defined density all along its length but this compound was successfully co-crystallized with the enzyme, while the other two were not. The diastereomers and **3** have more interactions with the amino acid side chains of dGMII, than do **2** and **4** (Table 2, see below) and these may explain the better resolved electron density.

Atoms making close contacts (<3.5 Å) with compound **6** are shown in Figure 2. The complex with **6** indicates that the hydroxyl groups on the five-membered ring interact with Asp 92, Asp 204, Asp 472, Tyr 727, Arg 876, and Zn in the enzyme active site. The hydroxyl groups on the aliphatic arm interact with Tyr 269, and Asp 340. The sulfate group on the side chain interacts with Arg 876. There are a number of water molecules that interact with the hydroxyl groups (OH-5, OH-2′, and OH-4′) and sulfate group. The selenonium center has a weak interaction (3.26 Å) with Asp 204. The Zn atom coordi-

Table 1. Refinement statistics

Compound	**2**	**3**	**4**	**5**	**6**
Common name	Salacinol	Ghavamiol	Seleno-salacinol	Diastereomer of salacinol	Diastereomer of seleno-salacinol
PDB code	1TQS	1TQU	1TQV	1TQT	1TQW
HET symbol	SSO	GHA	SSE	SSD	BLT
Data collection					
X-ray source	CHESS	OCI	OCI	OCI	CHESS
Wavelength (Å)	0.9504	1.54	1.54	1.54	0.9504
Cell dimensions (Å)	68.82/109.3/138.85	68.30/108.95/137.72	68.80/109.52/138.47	68.88/109.74/138.66	69.01/110.04/138.95
Data processing					
Resolution (Å) (overall/hi_res)	30–1.30/1.32–1.30	30–2.03/2.08–2.03	30–2.03/2.08–2.03	30–1.90/1.94–1.90	30–1.20/1.22–1.20
Reflections (unique/redundancy)	256,327/6.8	67,857/7.5	68,360/7.6	83,088/5.9	325,048/6.4
I/sigma (overall/hi_res)	14.5/5.4	40.2/9.7	25.7/5.4	20.0/5.5	23.3/2.3
% Completeness (overall/hi_res)	99.2/95.6	99.5/97.1	98.9/84.4	99.6/99.5	98.7/87.8
R Merge (overall/hi_res)	0.11/0.36	0.047/0.176	0.078/0.283	0.084/0.33	0.063/0.453
Refinement					
R_{test}/R_{free}	0.163/0.182	0.132/0.182	0.143/0.194	0.146/0.184	0.175/0.184
Amino acids	1014	1014	1014	1014	1014
Alternate conformations	17	23	13	18	33
Water molecules	1131	1132	1091	1019	1091
Rmsd bonds (Å)	0.021	0.022	0.014	0.018	0.021
Rmsd angles (°)	1.9	2.0	1.7	1.8	1.9
Average *B*-factor (Å^2)					
Overall	13.92	15.83	17.33	16.98	12.68
Protein main chain	10.94	12.92	14.49	14.24	10.25
Protein side chain	13.68	15.64	17.15	17.21	12.48
Water	25.05	26.57	28.01	26.67	21.69
Ligands	19.89	20.35	22.77	19.49	19.49

nates with the OD1 oxygen of Asp 204 and Asp 92, the NE2 nitrogen of His 90 and His 471, and OH-2, in a T_5 square pyramidal geometry (Fig. 2). This T_5 geometry matches with the square-based pyramidal geometry similar to that observed in the Tris–Zn complex (**1**) (Fig. 2). A summary of these bond distances for salacinol and its analogues, as well as for swainsonine (derived from PDB file 1HWW) is presented in Table 2. A stereoview of the overlay of the compound **6** complex with 1HWW is shown in Figure 2.

The corresponding structure of GMII with the nitrogen analogue ghavamiol (**3**) shows that the ring hydroxyl groups interact with Asp 92, Asp 204, Asp 472, Tyr 727, Arg 876, and Zn. The side chain, however, only interacts with Tyr 269 and Arg 228 through OH-2′ and is more free to move easily. The ammonium center has a strong interaction (2.99 Å) with Asp 204 (Fig. 2).

3. Discussion

We[6] and others[17] have recently reported the synthesis of salacinol **2** and its stereoisomers, for example, **5**, and we have also reported the syntheses of the hitherto unknown nitrogen, for example, **3** and selenium **4** and **6** congeners as potential glycosidase inhibitors.[7,9] Enzyme inhibition assays with a panel of glycosidase enzymes have indicated that the stereochemistry at the different stereogenic centers of the candidate inhibitors as well as the nature of the heteroatom play significant roles in discriminating between different glycosidase enzymes. It follows that alterations of the stereochemistry of centers, based on understanding of the atomic interactions between the compounds and their target enzymes, could be a powerful approach to the design of highly specific inhibitors.

Previous studies of this novel class of glycosidase inhibitor have focused on pancreatic α-amylase and intestinal α-glucosidases as possible mammalian physiological targets for inhibition.[4–6,9,18–21] In this work, we begin to address the salacinol-derived family of compounds as a starting point for a novel set of inhibitors of Golgi α-mannosidase II. Besides affinity itself, the specificity of inhibitors for GMII in preference to related enzymes, in particular the lysosomal mannosidase, is an important issue in limiting the side effects of any potential anti-metastatic or anti-inflammatory therapeutic.

The inhibitory activities of this series of compounds with α-amylases, glucoamylase, and intestinal glucosidases[7,9,19,22] has emphasized the importance of the stereochemistry at the centers on the heterocyclic ring as well as the stereochemistry at the centers on the sulfate-containing aliphatic arm in defining specificity. Therefore, these portions of the structures are presumed to make significant direct interactions with atoms in the enzyme active sites, or in defining critical structural or chemical characteristics of the ligands required for inhibition.

The observations reported in this study show that for GMII, interaction is mediated through the hydroxyl

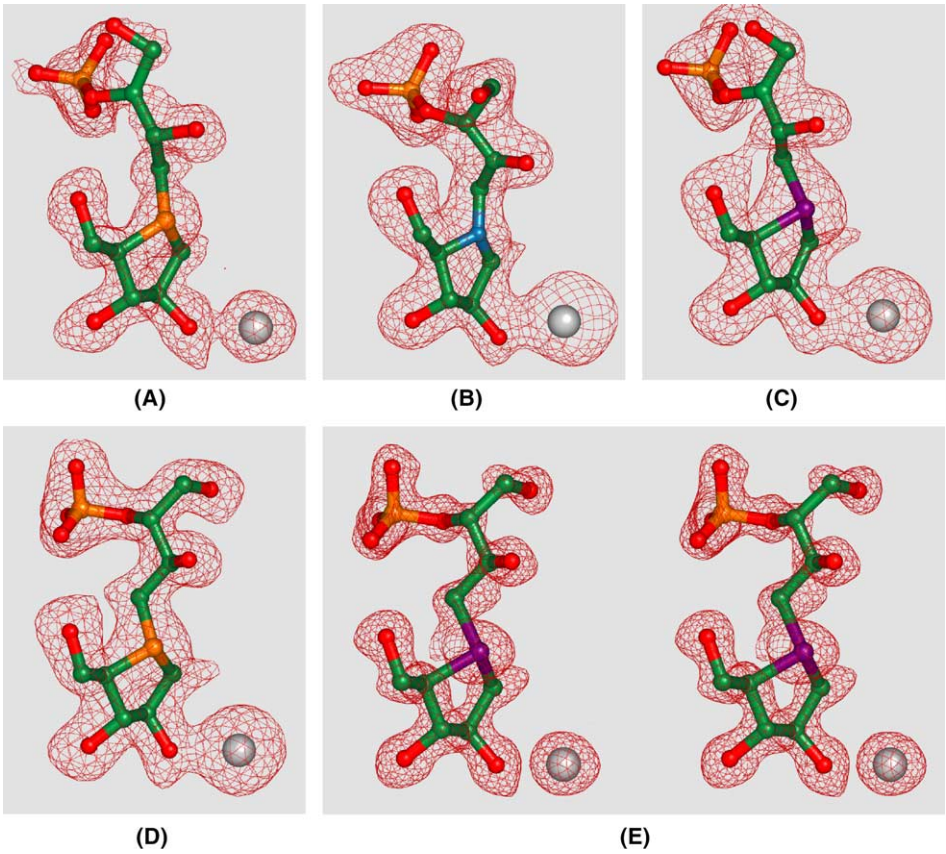

Figure 1. Electron density representations of the inhibitors under study. Maps are simulated annealing omit maps (F_o–F_c): (A) salacinol **2** contoured at 2.1σ (standard deviation); (B) ghavamiol **3** at 2.5σ; (C) seleno-salacinol (Blintol) **4** at 2.2σ; (D) salacinol diastereomer **5** at 2.5σ; (E) compound **6** at 2.5σ. For numbers in bold refer to Chart 1.

moieties on the five-membered, heterocyclic ring, and variations in the sulfate-containing arm have little effect on binding. This result is supported by inhibition data indicating that, for GMII, the stereochemistry of the hydroxyl groups in the heterocyclic ring is a crucial mediator of the interaction. Thus, for example, compounds corresponding to **3**–**6** in which the heterocyclic rings contained an enantiomeric orientation of the ring hydroxyl groups were inactive (data not shown). The enantiomeric conformation would result in the loss of critical interactions between the side chains of Tyr 727 and Asp 472 with the hydroxyl group at position 3, as well as between Zn with that at position 2 of the compounds (Fig. 2).

It is interesting to note that the conformations of the five-membered rings in the complexes of **3**–**6** display characteristics of the putative transition states in the catalytic mechanism. In particular, because of the intrinsic flexibility of the furanose ring, their conformation is largely dictated by the substituents, as guided by their interaction with the enzyme, rather than the ring energetics.[23] This allows us to view in the complexes, the positions of substituents as selected by the enzyme, presumably to stabilize the structure, unencumbered by any potential ring constraints, which should be more influential in six-membered pyranose ring systems. In addition, the transient positive charge of the transition state is mimicked by the permanent positive charge provided by the sulfonium, ammonium, or selenonium ions in these compounds. The interactions between these positive centers with the side chain of Asp 204, as also observed in the swainsonine complex,[1] are indicative of the electrostatic stabilization provided by the enzyme. For example, the selenonium center in compound **6** is located in a similar position to the nitrogen atom in swainsonine **1**. The hydroxyl groups OH-2, and OH-3 overlap very favorably with the OH-1, and OH-8 hydroxyl groups of swainsonine **1** (Fig. 2). The dominant electrostatic interactions in these inhibitors are with Asp 204 (Table 2). The fact that the selenium analogue **6** is only an inhibitor in the mM range whereas swainsonine **1** is a nM inhibitor might be a consequence of the closer electrostatic contact between charged centers (2.88 Å in **1** vs 3.12 Å in **6**). Thus, the mode of interactions that we report here for the salacinol family of compounds is consistent with an active site suited to stabilize a transition state predicted by the catalytic mechanism. The arguments presented here also suggest some advantages to designing inhibitors based on furanose, rather than pyranose, ring systems, in this situation.

Our results give some useful insights into the properties of the GMII active site and possible approaches to new inhibitors. The close interaction of the hydroxyl groups with the active site Zn atom reinforce our previous obser-

Table 2. Summary of interatomic distances (Å)

		1 Swainsonine		**2** Salacinol	**3** Ghavamiol	**4** seleno-salacinol	**5** Salacinol diastereomer	**6** Seleno-salacinol diastereomer
Zinc to:								
H90 NE2		2.14		2.08	2.05	2.06	2.09	2.07
D92 OD1		2.16		2.09	2.09	2.06	2.07	2.07
D204 OD1		2.16		2.07	2.15	2.20	2.17	2.07
H471 NE2		2.16		2.04	2.09	2.22	2.16	2.02
Inhibitor to:								
	Atom		Atom					
Zn	OH-1	2.31	OH-2	2.15	2.12	2.16	2.29	2.12
	OH-2	2.30						
D92 OD1	OH-2	2.91	OH-2	2.85	2.77	2.85	2.98	2.86
D92 OD2	OH-2	2.43	OH-2	2.98	3.02	3.03	2.98	3.07
D204 OD1	OH-1	2.83	OH-2	2.99	2.99	2.84	2.90	2.78
	N	2.88	S^+, N^+, or Se^+	S^+ 3.09	N^+ 2.99	Se^+ 3.14	S^+ 3.65	Se^+ 3.26
D204 OD2	N	3.55	S^+, N^+, or Se^+	S^+ 3.52	N^+ 3.74	Se^+ 3.14	S^+ 3.52	Se^+ 3.48
R228 NH2	—	—	OH-2′	3.49	2.67	3.28	—	—
Y269 OH	—	—	OH-2′	3.02	2.64	3.24	2.75	2.81
			S^+, N^+, or Se^+	S^+ 3.59	N^+ 4.03	Se^+ 3.25	S^+ 3.65	Se^+ 3.43
D340 OD1	—	—	OH-4′	—	—	—	2.54	2.65
D472 OD1	OH-8	2.51	OH-3	2.60	2.49	2.66	2.56	2.59
D472 OD2	OH-1	2.61	OH-2	2.58	2.31	2.47	2.47	2.55
Y727 OH	OH-8	2.69	OH-3	2.73	2.59	2.80	2.87	2.73
R876 O	—	—	OH-5	2.85	2.71	2.84	2.85	2.74
			SO	—	—	—	—	3.15
Waters			OH-5	2.62	2.66	2.68	2.72	2.68
			OH-2′	3.02	2.98	2.85	2.79	2.91
			OH-4′	—	2.71, 2.74, 3.05	—	2.71	2.64
			SO	2.62, 3.20, 3.09	2.71, 2.71, 3.03	2.75, 2.58, 2.94	2.57, 2.90, 3.02	2.92, 3.18

vations[1] of the importance of the Zn in binding substrate and transition state analogues. This unusual mechanism of interaction must be a major feature in any high affinity inhibitor. It also provides an opportunity to exploit this feature in newly-designed compounds.

It is of significance that with all our inhibitors **3**–**6**, the coordination with Zn is pentacoordinate or T_5, whereas with swainsonine **1**, the covalent intermediate, as formed with either 5-fluoro-gulose or 2-deoxy-2-fluoro-mannose, and pyranose-based inhibitors, it is hexacoordinate or T_6, with both OH-1 and OH-2 coordinating to the Zn atom.[1,2,24]

Compounds **3**–**6** and Tris, all have weak inhibitory activities toward GMII (in the millimolar range), in contrast with DMJ and swainsonine **1** (respectively, micromolar and nanomolar inhibitors). Presumably, the T_6 coordination of the Zn atom is present in the transition state (TS) of the glycosidase-mediated hydrolysis reaction. An effective TS mimic might therefore require T_6 coordination with Zn. These results taken together suggest that a high-affinity inhibitor of GMII should satisfy several criteria: a T_6 coordination with the Zn atom in the enzyme active site, good electrostatic contact with Asp 204, and a ring structure representative of the conformation reflected in the inhibitor complexes. The family of inhibitors discussed herein may be most informative on this last aspect.

The zinc coordination geometries T_4, T_5, and T_6 have been observed in proteins with frequencies of 48%, 44%, and 6%, respectively, for sites where the Zn ion is involved in catalysis, and 79%, 6%, and 12%, respectively, for sites in which Zn plays a structural role.[25] Thus, while T_6 sites occur rarely, T_5 is not an uncommon coordination in the context of enzyme active sites.[26–28] The entatic nature of zinc, permitting the alternative occupancies of coordination states observed in dGMII, is an important characteristic for this catalytic mechanism.

A further possible design feature derives from the lack of well-defined electron density for the side arms of some of the salacinol-based compounds, likely an indication of their flexibility and weak interaction with the GMII binding site. It is intriguing that in some of the compounds **3**, **5**, and **6**, the aliphatic arm is quite well

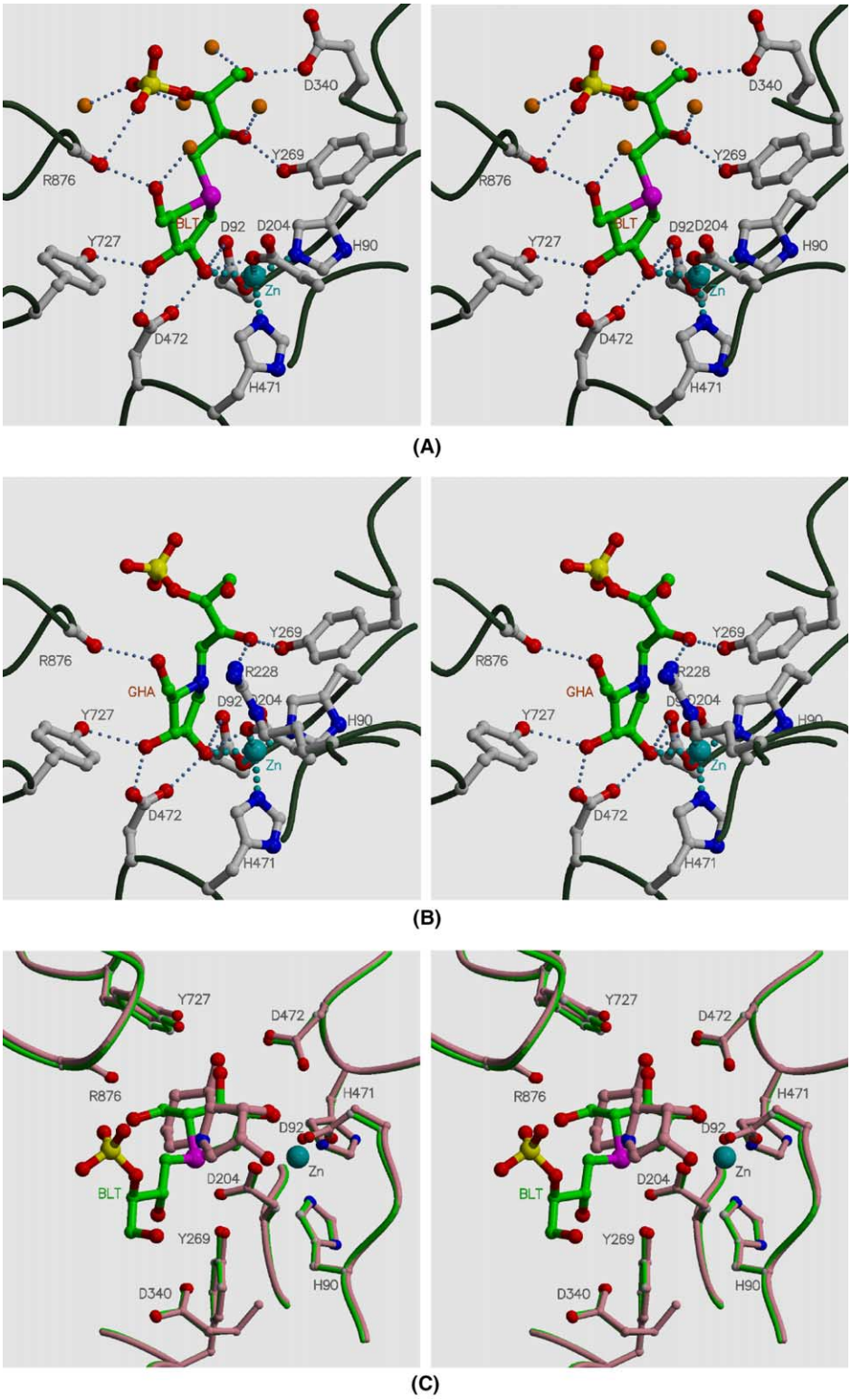

Figure 2. Divergent stereographs of the enzyme interactions with (A) compound **6** and (B) ghavamiol **3**, (C) overlay of **6** and swainsonine complexes.

ordered. Further refinement of the biased conformations that favor the well-defined structures, in combination with efforts to induce direct contacts between binding site residues and this side arm by incorporating the hydroxyl and sulfate groups into more rigid, cyclic structures, may also contribute to improved inhibitors.

4. Experimental techniques

The syntheses of the nitrogen **3**, and selenium **4** (Blintol) analogues of salacinol, a diastereomer **5**, and its corresponding selenium congener **6** used in this study have been reported previously (Chart 1).[6–9]

4.1. Inhibition assay

Inhibition of mannosidase activity was carried out in microtiter plates in a final volume of 50 μL. Inhibitors were dissolved in water to a final concentration of 200 mM. The reaction mixture consisted of 25 μL of 10 mM *para*-nitrophenol-α-mannoside (PNP–mannose), 10 μL of 200 mM buffer and 10 μL of water or inhibitor. The buffer used was MES pH 5.75 in the case of GMII (determined previously[10]) to be optimal for this enzyme. The reaction mixture was pre-warmed to 37 °C and 5 μL of mannosidase diluted in 10 mM Tris pH 8, 100 mM NaCl is added to initiate the reaction. The amount of enzyme added was that necessary to keep the reaction in the linear range. In the case of the GMII this represented approximately 350 ng of protein for a 15 min reaction. At the endpoint, the reaction was stopped using 50 μL of 0.5 M sodium carbonate. The absorbance of the reaction was measured at 405 nm with 520 nm background correction on a microtiter plate reader. One hundred percent activity was the activity of the enzyme in the absence of any inhibitor. Activity remaining was calculated as a percentage of this uninhibited activity and the value of 50% inhibition (IC_{50}) was taken from plots of remaining activity versus inhibitor concentration.

4.2. Crystallization

Crystallization of *Drosophila* Golgi mannosidase II was carried out using hanging drop vapor diffusion as described previously.[1] In all cases, crystals were less than 24 h old at the time of crystal evaluation and freezing. In the case of compounds **3** and **5** co-crystallization was successful in producing large well-diffracting crystals. Co-crystallization trials of the seleno-containing analogues **4** and **6** only produced showers of small crystals. For the latter compounds and for salacinol **2**, the crystals were grown in the absence of inhibitor and then soaked with inhibitor for approximately 30 min. Prior to freezing, the crystals were passed through drops containing 10%, 15%, 20%, and 25% 2-methyl-2,4-pentanediol. These cryo-solutions all contained 10 mM inhibitor. Inclusion of inhibitor in the cryo-solution was essential for visualizing clear electron density of these weakly binding compounds. Subsequent to cryo-solution exposure the crystals were mounted frozen in nylon CryoLoops (Hampton Research) directly in a liquid nitrogen cryostream.

4.3. Data collection

All data were collected at 100 K. Data were collected either at the Ontario Cancer Institute on a MAR Research 2300 image plate detector mounted on a rotating anode generator with Cu target, operated at 50 kV and 100 mA with beam focusing using Osmic optics, or at the Cornell High Energy Synchrotron Source, beamline F1 using an ADSC Quantum 4 CCD detector in the rapid readout mode. Typically 300–400 frames of 0.5° oscillation were collected for each data set. Data reduction and scaling were carried out using Denzo and Scalepack, respectively.[11]

4.4. Refinement

The software program CNS[12,13] has been used for the refinement of the structures of the complexes presented here. The structures of the complexes were solved by molecular replacement. Briefly, rigid body refinement was carried out against the published structure of native dGMII (PDB code 1HTY) with Tris and waters in the region of the active site removed. This was followed by simulated annealing to 3500 K, group *B*-factor refinement and individual *B*-factor refinement, prior to generation of electron density maps. At this initial stage *R*-factors were typically in the range of 22%, and the F_o–F_c density clearly shows the presence of bound compound and unassigned waters.

Refinement of the model involving manually fitting the compounds into the density, fitting waters, and checking side chains for proper fit to the density was carried out with O,[14] with intermittent rounds of energy minimization using CNS. Automated water-picking and deletion of weak waters were carried out using the automated routines from CNS, and the picked waters were checked manually. Once all waters and side chains were fit another round of simulated annealing and *B*-factor refinement was performed. Clear alternate conformations of side chains were then inserted, followed by energy refinement. Model correctness was checked with The MolProbity server (http://kinemage.biochem.duke.edu/molprobity) and the WhatIf server (http://www.biotech.ebi.ac.uk:8400/). Protein overlays and rmsd calculations were carried out using ProFit (http://www.bioinf.org.uk/software/profit). Graphics were generated using Pymol,[15] and Molscript.[16]

Acknowledgements

We thank the MacCHESS staff at the Cornell High Energy Synchrotron Facility for help with data collection. Supported by funding from the Canadian Institutes of Health Research (CIHR), and the Natural Sciences and Engineering Research Council of Canada (NSERC) Strategic Grants Program.

References

1. van den Elsen, J. M.; Kuntz, D. A.; Rose, D. R. *EMBO J.* **2001**, *20*, 3008–3017.
2. Numao, S.; Kuntz, D. A.; Withers, S. G.; Rose, D. R. *J. Biol. Chem.* **2003**, *278*, 48074–48083.
3. Koshland, D. E. J. *Biol. Rev. Camb. Philos. Soc.* **1953**, *28*, 416–436.
4. Yoshikawa, M.; Murakami, T.; Shimada, H.; Matsuda, H.; Yamahara, J.; Tanabe, G.; Muraoka, O. *Tetrahedron Lett.* **1997**, *38*, 8367–8370.
5. Yoshikawa, M.; Murakami, T.; Yashiro, K.; Matsuda, H. *Chem. Pharm. Bull.* **1998**, *46*, 1339–1340.
6. Ghavami, A.; Johnston, B. D.; Pinto, B. M. *J. Org. Chem.* **2001**, *66*, 2312–2317.
7. Ghavami, A.; Johnston, B. D.; Jensen, M. T.; Svensson, B.; Pinto, B. M. *J. Am. Chem. Soc.* **2001**, *123*, 6268–6271.

8. Svansson, L.; Johnston, B. D.; Gu, J.-H.; Patrick, B.; Pinto, B. M. *J. Am. Chem. Soc.* **2000**, *122*, 10769–10775.
9. Johnston, B. D.; Ghavami, A.; Jensen, M. T.; Svensson, B.; Pinto, B. M. *J. Am. Chem. Soc.* **2002**, *124*, 8245–8250.
10. Rabouille, C.; Kuntz, D. A.; Lockyer, A.; Watson, R.; Signorelli, T.; Rose, D. R.; van den Heuvel, M.; Roberts, D. B. *J. Cell Sci.* **1999**, *112*, 3319–3330.
11. Otwinowski, Z.; Minor, W. *Methods Enzymol.* **1997**, *276*, 307–326.
12. Brunger, A. T.; Adams, P. D. *Acc. Chem. Res.* **2002**, *35*, 404–412.
13. Brunger, A. T.; Adams, P. D.; Clore, G. M.; DeLano, W. L.; Gros, P.; Grosse-Kunstleve, R. W.; Jiang, J. S.; Kuszewski, J.; Nilges, M.; Pannu, N. S.; Read, R. J.; Rice, L. M.; Simonson, T.; Warren, G. L. *Acta Crystallogr. D—Biol. Crystallogr.* **1998**, *54*, 905–921.
14. Jones, T. A.; Zhou, J. Y.; Cowan, S. W.; Kjeldgaard, M. *Acta Crystallogr.* **1991**, *A47*, 110–119.
15. DeLano, W. L. *The PyMol Molecular Graphics System*; DeLano Scientific: San Carlos, CA, USA, 2002.
16. Kraulis, P. J. *J. Appl. Crystallogr.* **1991**, *24*, 946–950.
17. Yuasa, H.; Takada, J.; Hashimoto, H. *Tetrahedron Lett.* **2000**, *41*, 6615–6618.
18. Yoshikawa, M.; Morikawa, T.; Matsuda, H.; Tanabe, G.; Muraoka, O. *Bioorg. Med. Chem.* **2002**, *10*, 1547–1554.
19. Ghavami, A.; Johnston, B. D.; Maddess, M.; Chinapoo, S. M.; Jensen, M. T.; Svensson, B.; Pinto, B. M. *Can. J. Chem.* **2002**, *80*, 937–942.
20. Muraoka, O.; Ying, S.; Yoshikai, K.; Matsuura, Y.; Yamada, E.; Minematsu, T.; Tanabe, G.; Matsuda, H.; Yoshikawa, M. *Chem. Pharm. Bull.* **2001**, *49*, 1503–1505.
21. Wolf, B. W.; Weisbrode, S. E. *Food Chem. Technol.* **2003**, *41*, 867–874.
22. Pinto, B. M., et al., unpublished.
23. Lehmann, J. George Thieme: Stuttgart, 1998; pp 31–33.
24. Shah, N.; Kuntz, D. A.; Rose, D. R. *Biochemistry* **2003**, *42*, 13812–13816.
25. Alberts, I. L.; Nadassy, K.; Wodak, S. J. *J. Protein Sci.* **1998**, *7*, 1700–1716.
26. Auld, D. S. *BioMetals* **2001**, *14*, 271–313.
27. Harding, M. M. *Acta Crystallogr.* **2001**, *D57*, 401–411.
28. Harding, M. M. *Acta Crystallogr.* **2004**, *D60*, 849–859.